NASA Technical Memorandum 102423

Strength and Toughness of Monolithic and Composite Silicon Nitrides

Jonathan A. Salem
Lewis Research Center
Cleveland, Ohio

January 1990

NASA

STRENGTH AND TOUGHNESS OF MONOLITHIC AND COMPOSITE SILICON NITRIDES*

Jonathan A. Salem
National Aeronautics and Space Administration
Lewis Research Center
Cleveland, Ohio 44135

SUMMARY

The strength and toughness of two composite and two monolithic silicon nitrides were measured from 25 to 1400 °C. The monolithic and composite materials were made from similar starting powders. Both of the composite materials contained 30 vol % silicon carbide whiskers. All measurements were made by four-point flexure in surrounding air and humidity. The composite and monolithic materials exhibited similar fast fracture properties as a function of temperature.

INTRODUCTION

The need for more fuel efficient transportation and lower engine emissions has made ceramics increasingly important structural materials. Ceramics offer many beneficial properties, such as high-temperature strength, low density, and low thermal conductivity. However, they exhibit low toughness and low reliability.

One approach that may improve the toughness, crack growth resistance and reliability of monolithic silicon nitride is the addition of whiskers or fibers. Whiskers may bridge developing cracks and thereby impart toughness, crack growth and creep resistance. The objective of this work was to determine properties and structural behavior of developmental silicon carbide whisker reinforced silicon nitrides. Similar monolithic materials were also studied to provide a general base of comparison.

MATERIALS PROCESSING AND MECHANICAL PROPERTIES

Materials Processing

The materials used in this study were based on Garrett's GN-10 and a Norton monolithic silicon nitride. At the time of this study, composite versions were not commercially available, however, limited quantities had been processed.

Garrett Company GN-10 silicon nitride powder composition was slip cast into 50 mm diameter, 75 mm height billets, glass encapsulated by the ASEA[1] method and HIPed to produce monolithic material. Part of the same powder

---

*Prepared for Oak Ridge National Laboratory's Ceramic Technology for Advanced Heat Engines Project, Interagency Agreement DE-AI05-87OR21749, W.B.S. Element 3.2.1.7.

[1]ABB Autoclave Systems, Columbus, Ohio.

batch was blended with 30 vol % SiC whiskers by ACMC[2] and processed with the same procedures as the monolithic. Densities of the monolithic and composite materials were 3.31 and 3.27 g/cm^3, respectively.

The Norton Company based materials were processed by mixing silicon powder with 4 wt % Y_2O_3 and then adding 30 vol % Tateho T44 SiC whiskers to a portion of the powders. The powder mixtures were cast as a slurry into 50 mm square by 6 mm thick plates, cold isostatically pressed, nitrided, and HIPed by the ASEA glass encapsulation method. Densities of the monolithic and composite materials were 3.24 and 3.23 g/cm^3, respectively.

Machining and Nondestructive Evaluation

Strength and fracture toughness specimens were machined from billets of Garrett material with the longitudinal axis perpendicular to the billet diameter. Specimens from the Norton materials were machined with the 3 mm dimension parallel to the hot pressing direction of the plates.

Test specimens were inspected using radiography, optical microscopy and ultrasonic evaluation. Specimens were radiographed through the thickness and width at several intensities and times to produce optimum conditions. Optical inspection was performed with a machinists scope from 10× to 50×. Precision ultrasonic measurements were performed with an automated system at 50 MHz (ref. 1).

Mechanical Testing

Four-point bend strength was determined in accordance with MIL Standard 1942 (ref. 2) at temperatures from 25 to 1400 °C. Between three and ten specimens were tested per temperature. The specimens measured 3 by 4 mm in thickness and width and were tested with spans of 20 and 40 mm (size B). The nature and location of failure origins was determined with optical microscopy or scanning electron microscopy.

Fracture toughness was determined by the chevron-notch method (ref. 3). Because of slight variations in the notch geometry, the stress intensity factor coefficients were determined with the straight-through crack assumption (ref. 3). Specimens measured 3 by 6 mm in thickness and width, with 20 and 40 mm spans. Three to six specimens were tested per temperature. The specimens were tested at a stroke rate of 0.05 mm/min. The low stroke rate used for chevron-notch testing was required to insure stable crack extension.

RESULTS AND DISCUSSION

Nondestructive Evaluation

The Garrett monolithic material exhibited a coarse cellular structure that was visible to the unaided eye and in radiographs. The composite

---

[2]Advanced Composite Materials Corp., Greer, South Carolina.

occasionally exhibited the same macro-cellular structure and a banding or chemical layering, figure 1, in the radial direction, similar to the billet geometry (a cylinder). This may have resulted from shrinkage during the slip casting process. Such radiographic observations have been related to density variations (ref. 4). However, ultrasonic velocity measurements, which are sensitive to density variations, were similar for regions of radiographic dissimilarity, indicating chemical, rather than density variations. Attempts to determine compositional differences via energy dispersive analysis and electron microphobe scans were fruitless. However, dye penetrant tests indicated the cell boundaries to contain fine disconnected porosity.

Very little anisotropy (less than 1 percent) in composite or monolithic billets of Garrett material could be detected with velocity measurements in longitudinal and transverse directions, as shown in table I. Velocity measurements on samples machined from different billets also showed little difference (table II). The velocity as a function of longitudinal position was also determined to be similar for the center 2 cm of two billets (table III).

Radiography of the Norton material indicated the composite to be homogeneous. However, the monolithic material had significant density or compositional variations on one 50 mm face of the plates (fig. 2). Acoustic microscopy was not performed on the Norton materials. Electron microprobe scans indicated some concentrations of yttrium and a few regions of tungsten concentration. No significant edge-to-edge chemical differences were determined.

Bend Strength

A summary of bend strength and fracture toughness test results is given in table IV. Strength of the Garrett composite and monolithic materials were similar at each test temperature (fig. 3).

In contrast, the Norton composite exhibited higher strength than the corresponding monolithic at 25, 800, and 1200 °C, and similar strength at 1000 and 1400 °C (fig. 3). The low room temperature strength of the monolithic was attributed to the aforementioned density variations.

Fracture Toughness

Fracture toughnesses of the Garrett composite and monolithic materials were comparable as a function of temperature (fig. 4). Fracture toughness, calculated from maximum load and minimum stress intensity coefficient, decreased with temperature to 1200 °C. However, at 1400 °C the observed toughness increased substantially. Evidently the combination of slow stroke rate and high temperature resulted in creep deformation during crack extension. For such temperatures, toughness measurements determined with chevron-notches can be much higher than those made with precracked beams (ref. 5). Thus, chevron-notches may be inappropriate for such high temperatures.

The Norton composite and monolithic materials exhibited similar toughnesses as a function of temperature; toughness increased from a minimum at room temperature to a maximum at 1000 °C, and decreased through 1400 °C (fig. 4). This brittle room temperature behavior, followed by intermediate temperature toughening, was attributed to softening of glass in the grain

boundary phase. Continued glass softening resulted in decreasing strength and toughness above 1000 °C.

Fractography and Microscopy

Typical microstructures are illustrated in figures 5 and 6. The whisker distribution in the Garrett composite was somewhat heterogeneous, with the whiskers distributed randomly in some regions and oriented in others. Whiskers, shown in figure 7, were revealed with a modified plasma etching procedure (ref. 6). The procedure did not work well on the Norton material because of the short whisker lengths.

TEM observations of the monolithic and composite Norton materials indicated grain-boundaries with significant crystallization. The crystallized grain boundaries were Y-rich, but the phases could not be identified. Glassy regions remained, some of which were phase separated. These regions were low in yttrium content, but had accumulated many impurities, e.g., K, Ca, Cl, Na, P, S, etc. thought to be from abrasion of a rubber mill seal during processing. The glassy regions also contained small, spherical W-rich particles, presumably from milling media. Many Si_3N_4 grains contained dislocations. The composite material contained large SiC grains, which were debris added with the SiC whiskers (Norton is taking steps to remove large chunks from whiskers). Many of the whiskers were hollow and contained Y-rich amorphous phases and small Si_3N_4 crystals. The SiC whiskers were bonded to the matrix by a glassy phase, which explained the lack of significant whisker pull-out observed on room temperature fracture surfaces, shown in figure 8.

Fracture surfaces of both composite materials did exhibit whiskers and their impressions. The size of exposed whiskers and impressions were typically on the same order as the grains and agglomerates. However, large extensions of fibers were occasionally observed (fig. 8). To attain toughening via whisker additions, the fibers may have to act over dimensions greater than the grain and agglomerate size.

The Garrett materials failed from porous regions, coarse grained regions, and agglomerates (fig. 9). The failure initiating flaws in the Norton monolithic were subsurface porous areas 30 to 60 μm across (fig. 10).

The Norton composite failed from SiC chunks of approximately 50 μm length. The size of the failure origins were much greater than whisker lengths, and strength improvements can only be expected if the fibers are capable of bridging such flaws, or stabilizing cracks that extend from them.

SUMMARY OF RESULTS

The addition of 30 vol % SiC whiskers to monolithic silicon nitrides did not substantially improve room or elevated temperature strength or toughness. Silicon carbide chunks occasionally acted as failure origins in both composite materials. Whiskers and remnant impressions on the order of grain size where typically visible, however, well extended fibers were only occasionally visible. Either different whiskers, different bonding, or improved microstructures may be required to improve the fracture properties via whisker additions.

ACKNOLEDGEMENTS

The author would like to thank ORNL for funding, and T. Leonhardt, D. Stang, S. Klima, and Dr.'s E. Generazio, S. Levine, and J. Gyekenyesi for assistance that made this report possible.

REFERENCES

1. Generazio, E.R.; Roth, D.J.; and Baaklini, G.Y.: Acoustic Imaging of Subtle Porosity Variations in Ceramics. Mater. Eval., vol. 46, no. 10, Sept. 1988, pp. 1338-1343.

2. High Performance Ceramics at Ambient Temperature. MIL-STD-1942, Nov. 21, 1983.

3. Munz, D.; Bubsey, R.T.; and Shannon, J.L., Jr.: Fracture Toughness Determination of Al_2O_3 Using Four-Point-Bend Specimens with Straight-Through and Chevron Notches. J. Am. Ceram. Soc., vol. 63, no. 5-6, May-June 1980, pp. 300-305.

4. Generazio, E.R.; Stang, D.B.; and Roth, D.J.: Dynamic Porosity Variations in Ceramics. NASA TM-101340, 1988.

5. Salem, J.A., et al.: Elevated Temperature Strength, Toughness, and Elastic Modulus of a Silicon Nitride Combustor. NASA TM- , to be published, 1990.

6. Siebein, K.N.; and Lovington, W.M.: Plasma Etching of Si_3N_4. Microstructural Science, Vol. 16, Metallography of Advanced Materials, J.H. Cialone, et al., eds., ASM International, Metals Park, OH, 1988, pp. 319-329.

TABLE I. - ULTRASONIC SHEARWAVE VELOCITIES IN THE TRANSVERSE AND LONGITUDINAL DIRECTIONS OF MOR BARS OF GARRETT MATERIALS

Billet or specimen	Velocity, cm/μs (longitudinal)	Velocity (transverse)
C-2/03	0.628	[a]0.626
C-3/03	.624	[a].624
C-11/05	.631	[a].632
C-12/04	.627	[a].628
M-1/01	.601	[b].601

[a]Composite.
[b]Monolithic.

TABLE II. - ULTRASONIC VELOCITIES IN GARRETT BILLETS

Billet (composite)	Velocity, cm/μs	Billet (monolithic)	Velocity, cm/μs
C-12	1.082	M-1	1.081
C-11	1.092	M-2	1.082
C-8	1.083	M-3	1.088
C-3	1.075	M-C	1.082
C-2	1.082	---	-----

TABLE III. - VARIATION OF ULTRASONIC VELOCITY ALONG THE LENGTH OF MONOLITHIC AND COMPOSITE GARRETT BILLETS

Distance from center, cm	Velocity, cm/μs	
	Monolithic	Composite
-1.0	1.084	1.082
-0.5	1.083	1.083
0.0	1.081	1.082
+0.5	1.077	1.082
+1.0	1.077	1.082

TABLE IV. - STRENGTH AND TOUGHNESS WITH STANDARD DEVIATION

Material	Temperature, °C				
	25	800	1000	1200	1400
Strength MPa					
Garrett					
Si_3N_4	732±61	715±52	679±15	617±35	405±68
SiC/Si_3N_4	698±85	671±45	702±14	628±44	344±27
Norton					
Si_3N_4	550±82	531±67	585±40	535±109	336±36
SiC/Si_3N_4	758±66	648±95	562±362	693±31	370±6
Toughness $MPa \cdot m^{1/2}$					
Garrett					
Si_3N_4	6.5±.3	6.5±.4	5.7±.5	5.8±.4	10.1±1.3
SiC/Si_3N_4	7.1±.5	5.6±.2	6.2±.1	5.7±.4	10.7±.4
Norton					
Si_3N_4	4.3±.3	4.4±.2	6.5±.7	6.3±.1	5.9±.1
SiC/Si_3N_4	4.9±.2	5.4±1	6.2±.1	5.9±.1	5.7±1.4

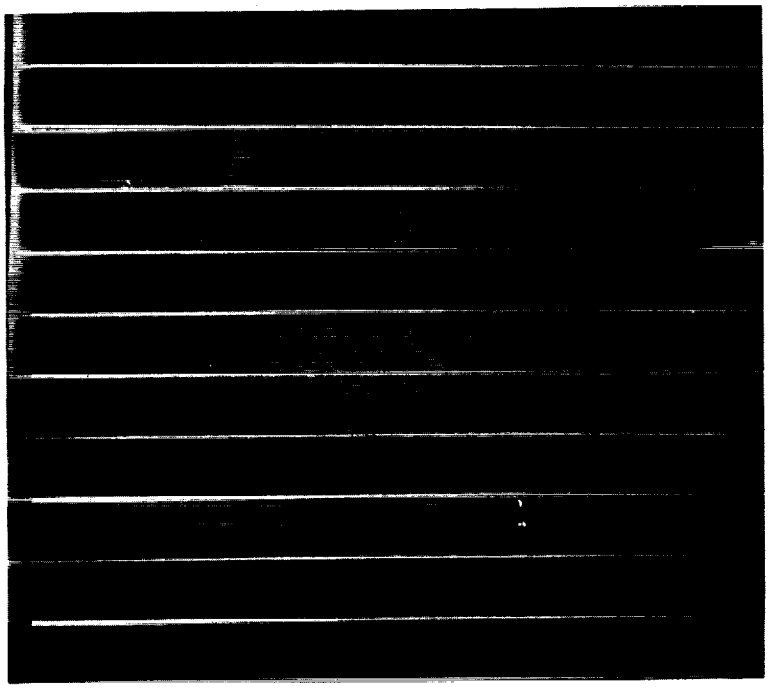

(a) SiC_w/Si_3N_4

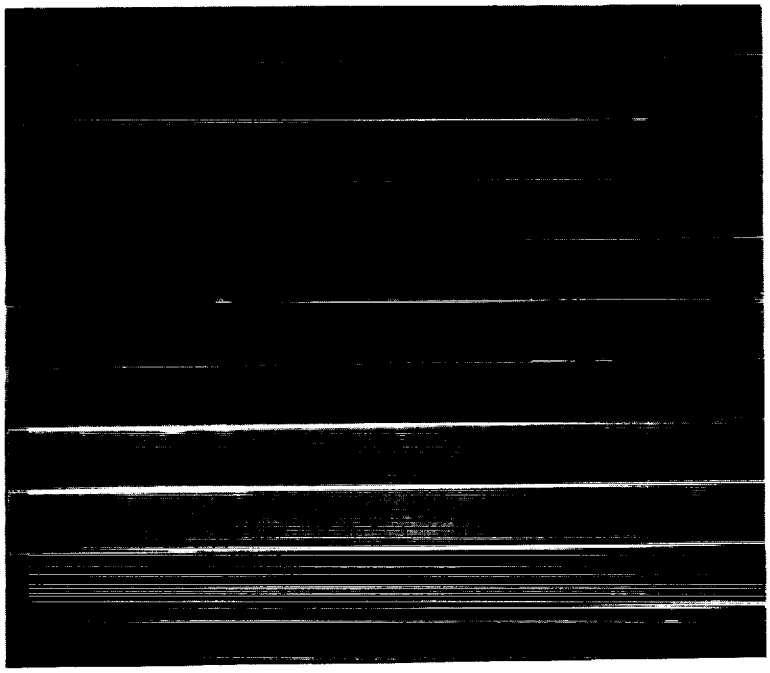

(b) Si_3N_4.

Figure 1. - X-ray radiographs of MOR bars machined from cylindrical billets of Garrett materials. Dark zones imply higher density or constituents with greater x-ray absorption.

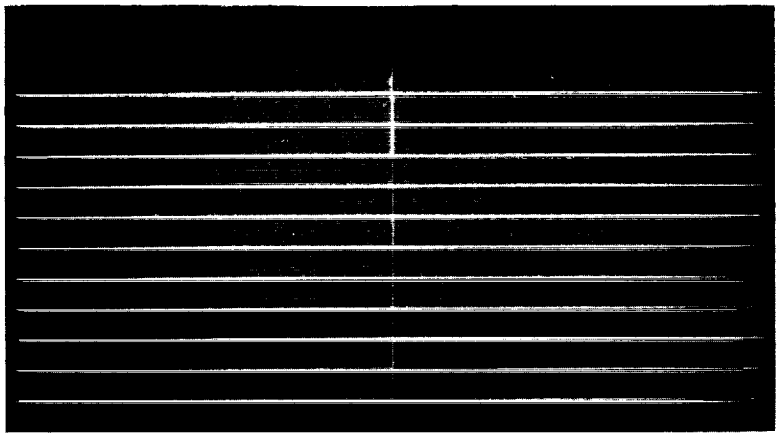

(a) SiC_w/Si_3N_4.

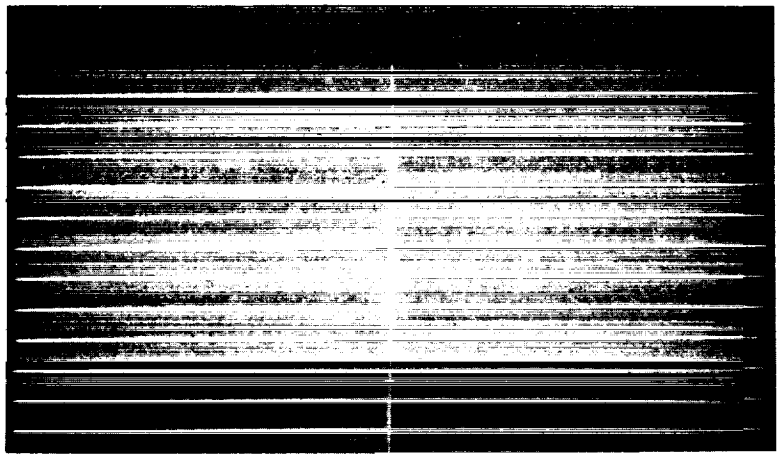

(b) Si_3N_4.

Figure 2. - X-ray radiographs of MOR bars machined from plates of Norton materials. Dark zones imply higher density or constituents with greater x-ray absorption.

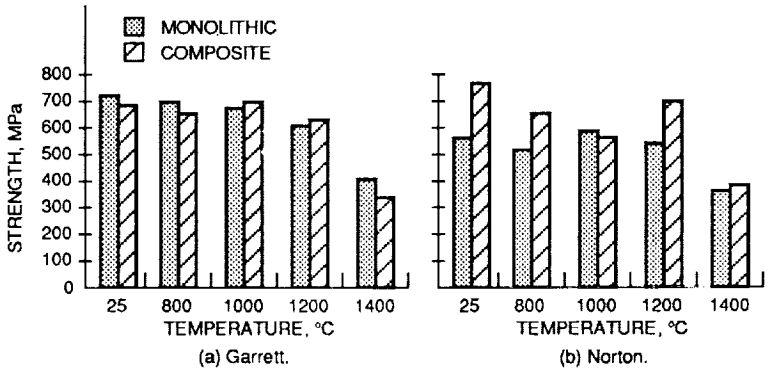

(a) Garrett. (b) Norton.

Figure 3. - Four-point bend strength of Si_3N_4 and SiC_w/Si_3N_4 materials.

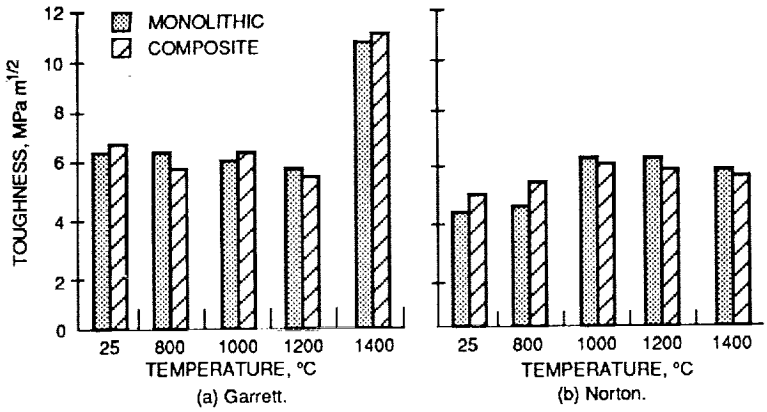

Figure 4. - Fracture toughness of Si_3N_4 and SiC_w/Si_3N_4 materials.

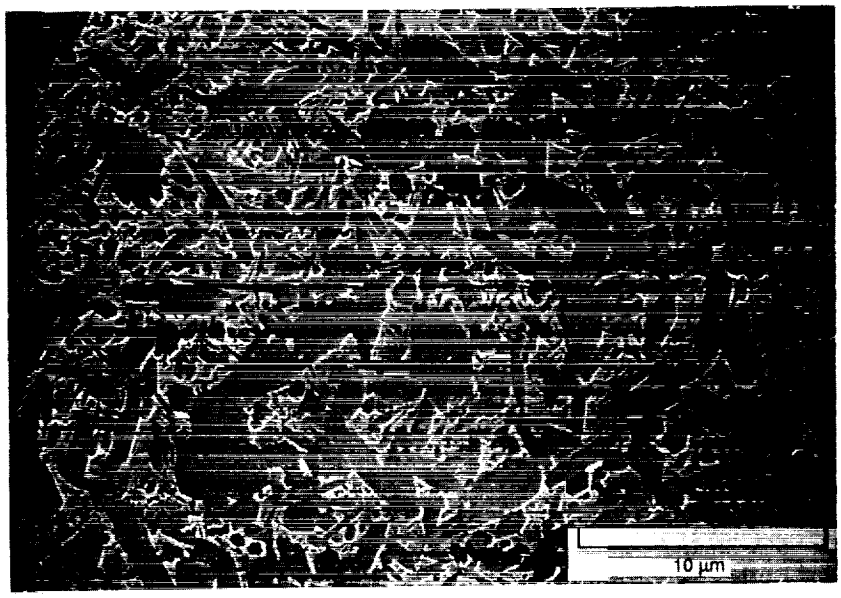

(a) Si_3N_4.

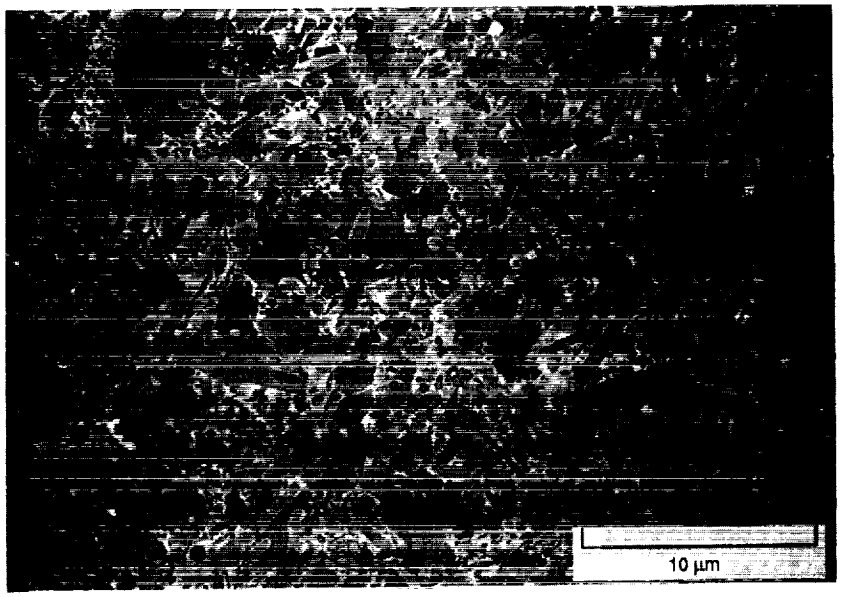

(b) SiC_w/Si_3N_4.

Figure 5. - Microstructure of Garrett materials: where darkest regions are Si_3N_4, grey regions are SiC whiskers, and light regions are intergranular phase.

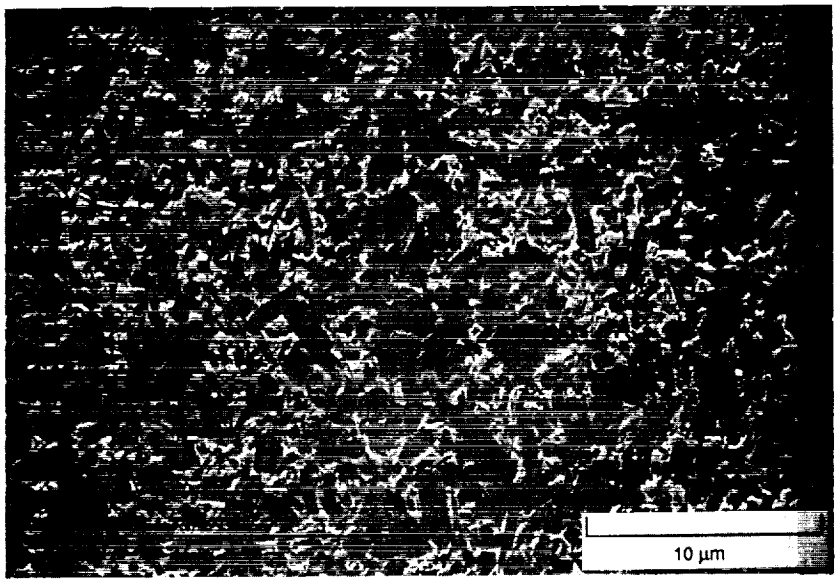

(a) Si_3N_4.

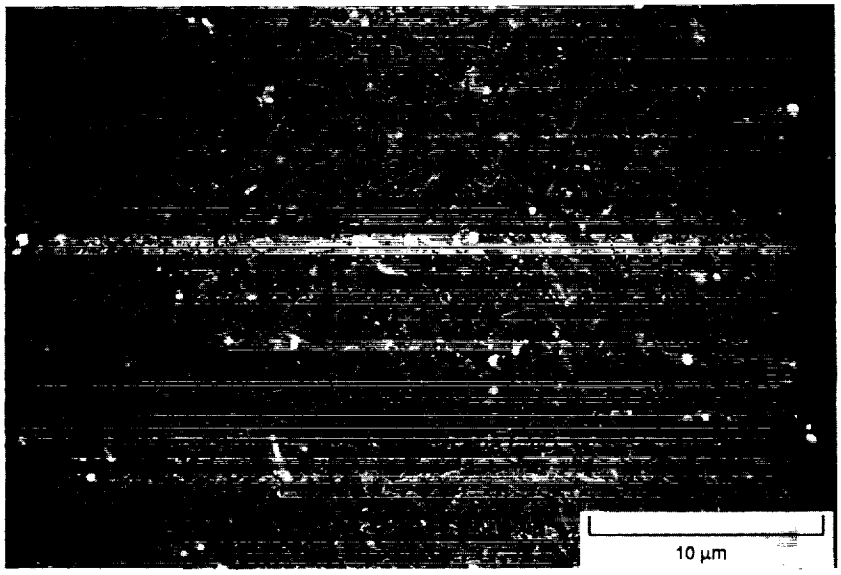

(b) SiC_w/Si_3N_4.

Figure 6. - Microstructure of Norton materials: where darkest regions are Si_3N_4, grey regions are SiC whiskers, and light regions are interangular phase.

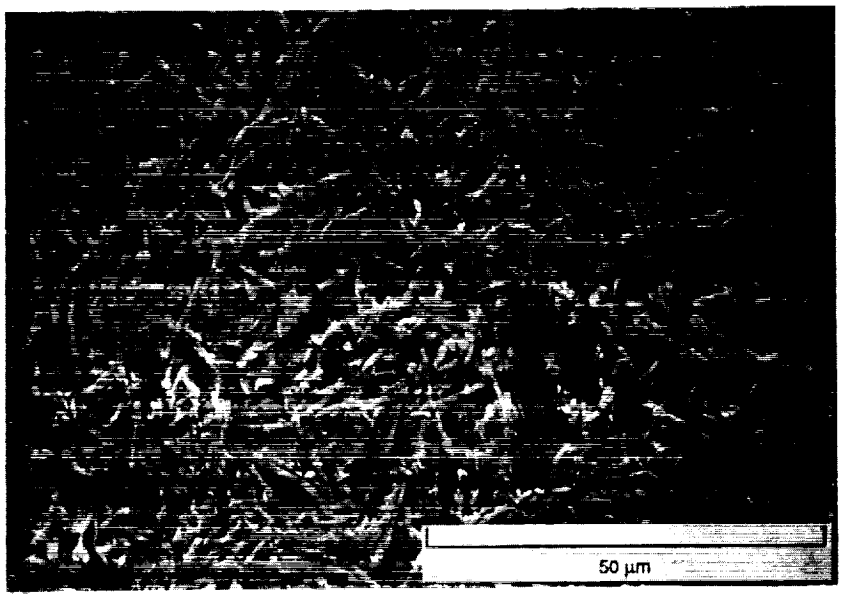

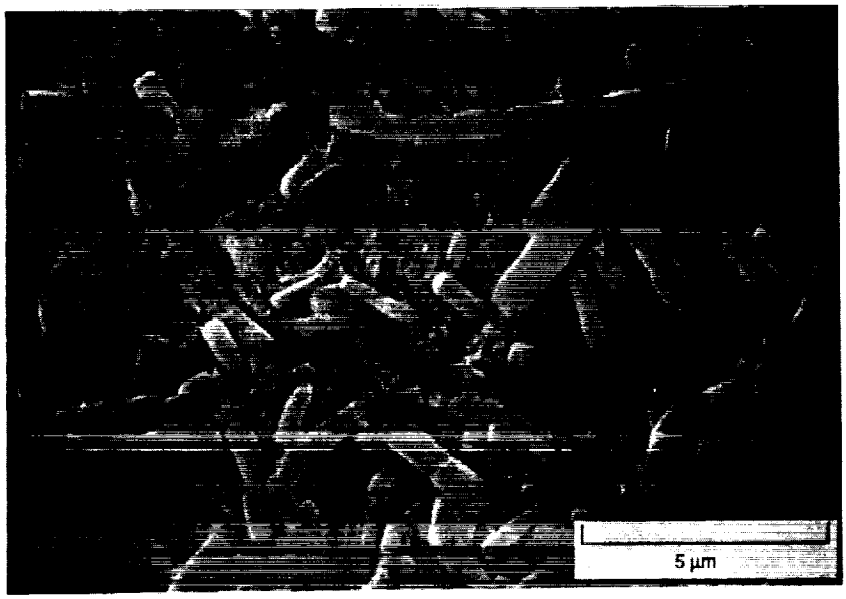

Figure 7. - Whiskers in Garrett SiC_w/Si_3N_4 exposed via plasma etching.

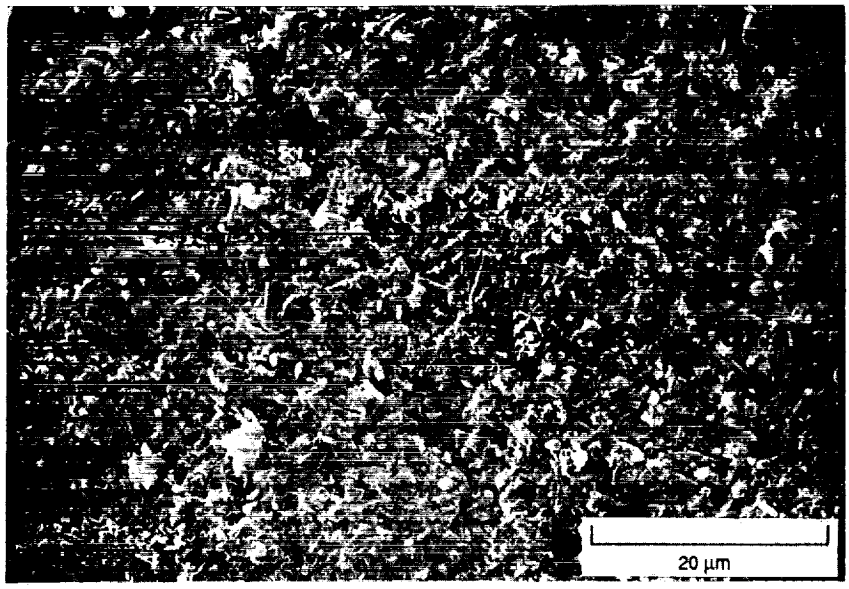

(a) Garrett.

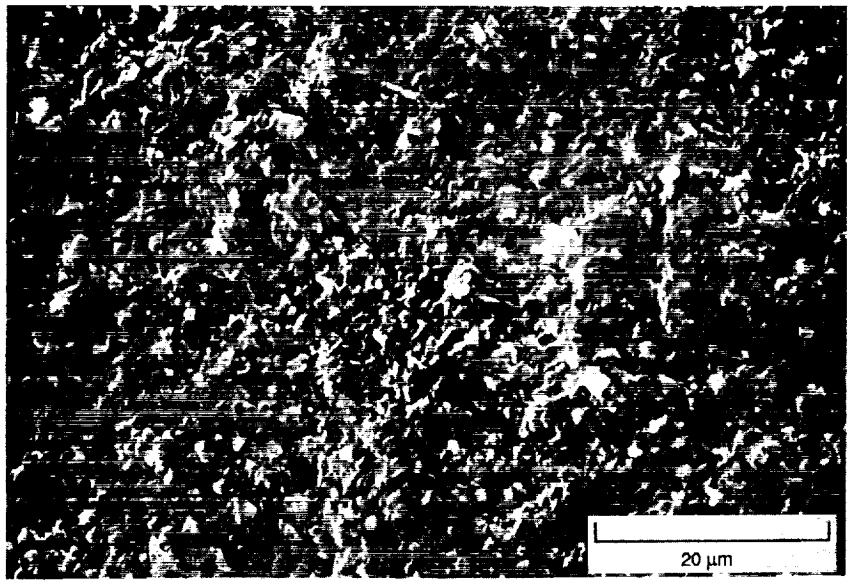

(b) Norton.

Figure 8. - Fracture topography of SiC_w/Si_3N_4 fracture toughness specimens (25 °C).

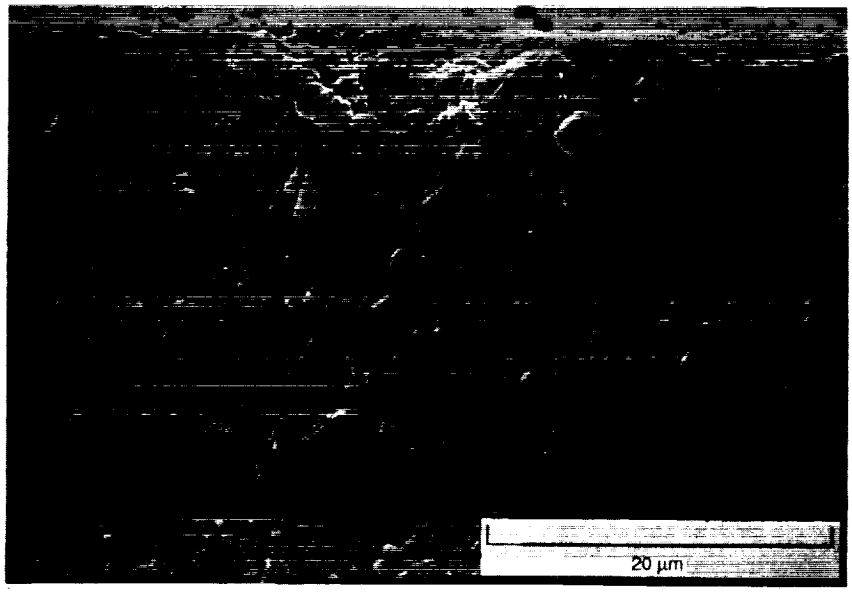

(c) Whisker pullout around a failure origin in Garrett composite.

Figure 8. - Concluded.

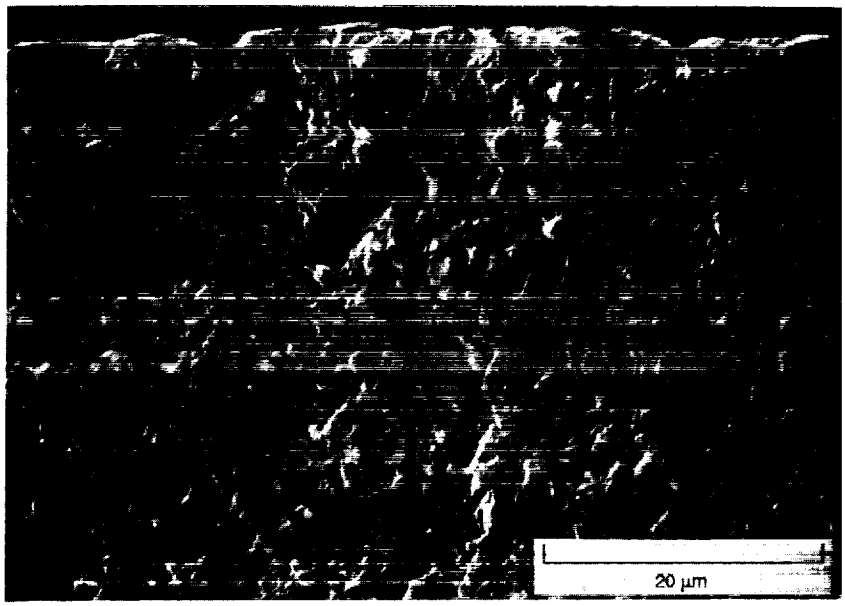

(a) Coarse grained region (monolithic).

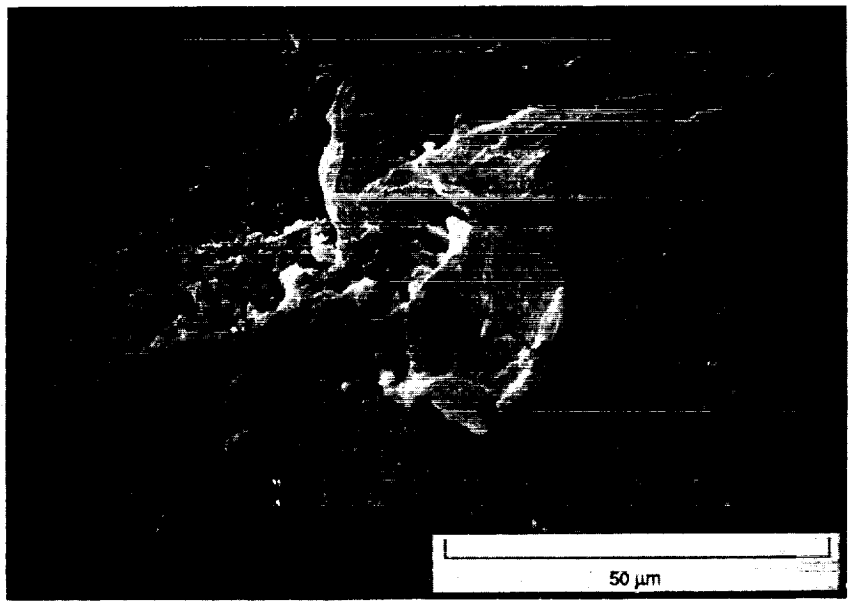

(b) Agglomerate (monolithic).

Figure 9. - Failure origins in the Garrett materials.

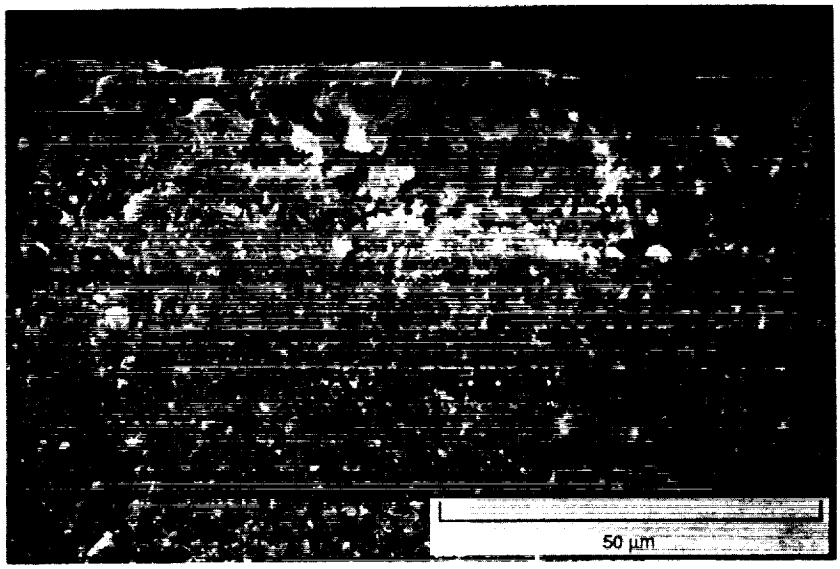

(c) Porous region (composite).

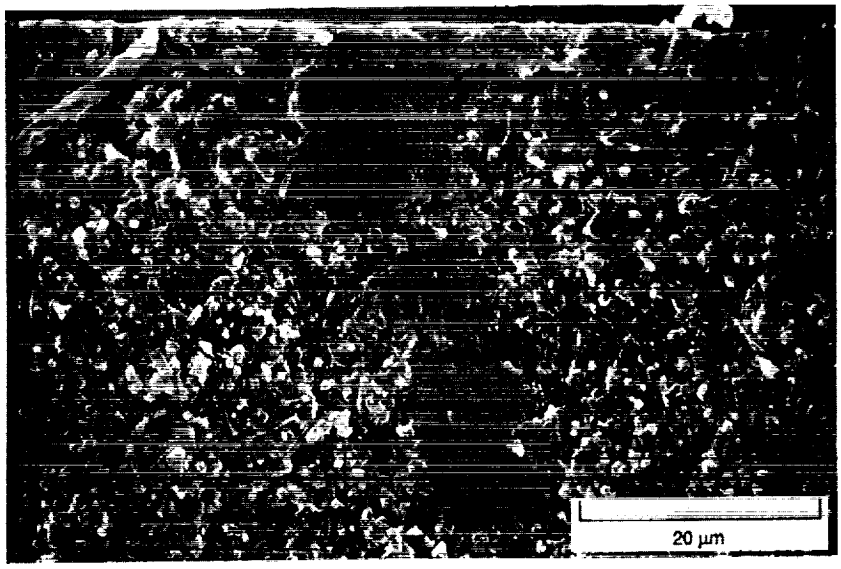

(d) Agglomerate (composite).

Figure 9. - Concluded.

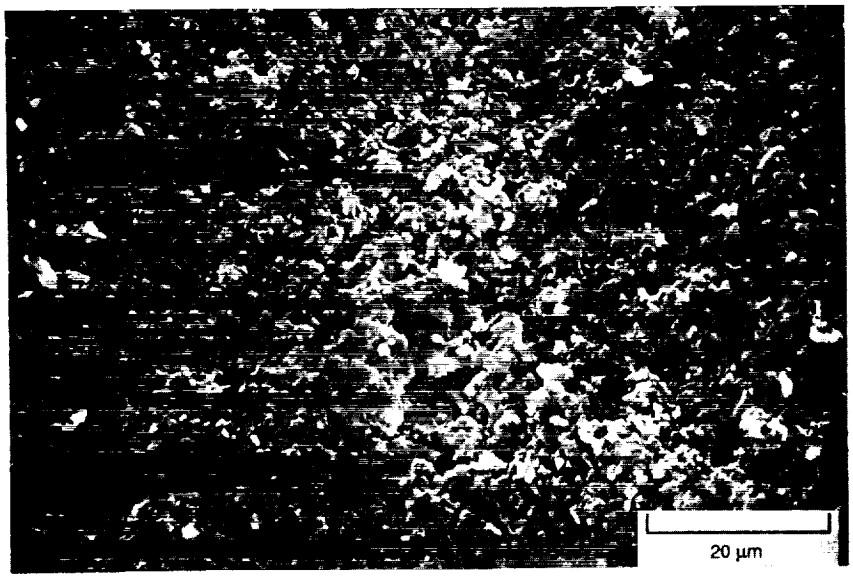

(a) Porous regions (monolithic).

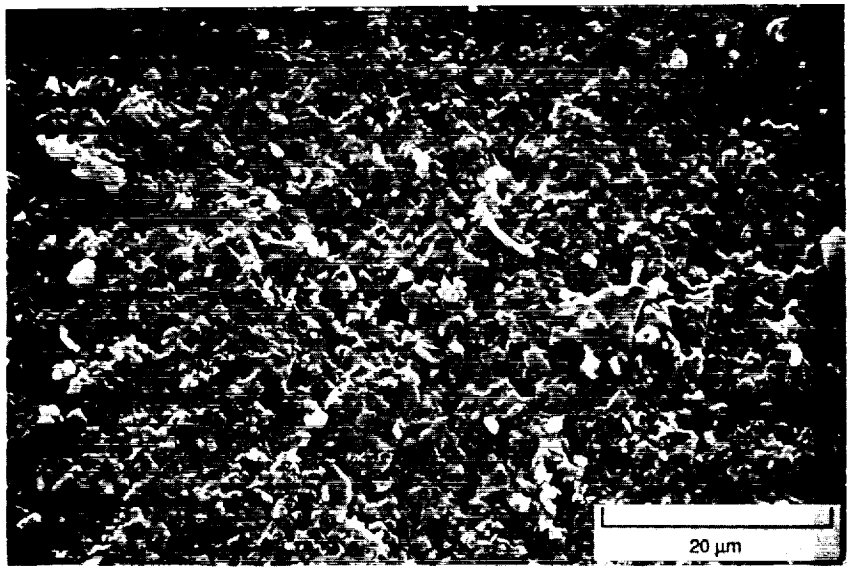

(b) Porous regions (monolithic).

Figure 10. - Failure origins in the Norton materials.

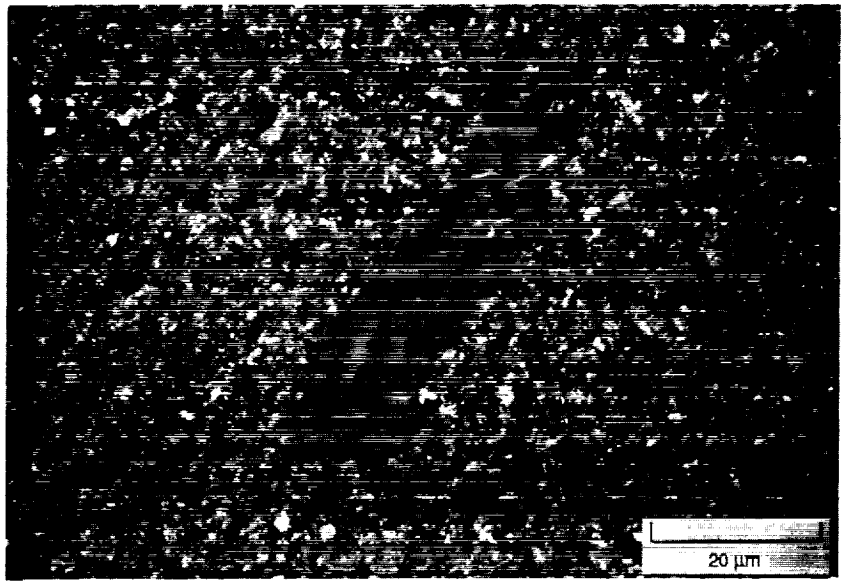

(c) SiC chunk (composite).

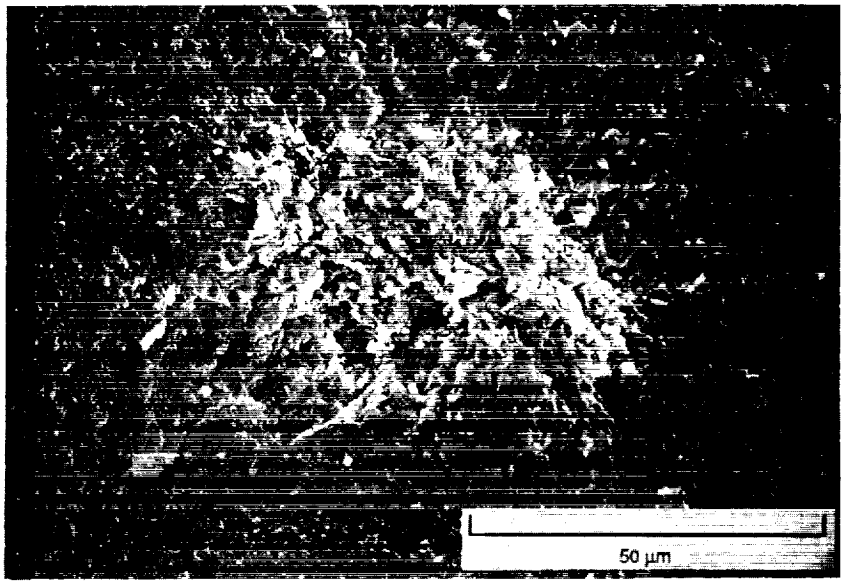

(d) Agglomerate (composite).

Figure 10. - Concluded.

NASA
National Aeronautics and Space Administration

Report Documentation Page

1. Report No.	2. Government Accession No.	3. Recipient's Catalog No.
NASA TM-102423		

4. Title and Subtitle	5. Report Date
Strength and Toughness of Monolithic and Composite Silicon Nitrides	January 1990
	6. Performing Organization Code

7. Author(s)	8. Performing Organization Report No.
Jonathan A. Salem	E-5188
	10. Work Unit No.
	505-63-IM

9. Performing Organization Name and Address	11. Contract or Grant No.
National Aeronautics and Space Administration Lewis Research Center Cleveland, Ohio 44135-3191	
	13. Type of Report and Period Covered
	Technical Memorandum

12. Sponsoring Agency Name and Address	14. Sponsoring Agency Code
National Aeronautics and Space Administration Washington, D.C. 20546-0001	

15. Supplementary Notes

Prepared for Oak Ridge National Laboratory's Ceramic Technology for Advanced Heat Engines Project. Interagency Agreement DE-AI05-87OR21749, W.B.S. Element 3.2.1.7.

16. Abstract

The strength and toughness of two composite and two monolithic silicon nitrides were measured from 25 to 1400 °C. The monolithic and composite materials were made from similar starting powders. Both of the composite materials contained 30 vol % silicon carbide whiskers. All measurements were made by four-point flexure in surrounding air and humidity. The composite and monolithic materials exhibited similar fast fracture properties as a function of temperature.

17. Key Words (Suggested by Author(s))	18. Distribution Statement
Strength; Fracture toughness; Silicon nitride; Composites; Elevated temperature	Unclassified – Unlimited Subject Category 27

19. Security Classif. (of this report)	20. Security Classif. (of this page)	21. No of pages	22. Price*
Unclassified	Unclassified	20	A03

NASA FORM 1626 OCT 86

*For sale by the National Technical Information Service, Springfield, Virginia 22161